Inorganica Chimica Acta, 182 (1991) 221-228

Heterobimetallic aggregates derived from the double cubane-like structure $(NMe_4)_4[MS_4(CuCl)_5Cl_2]$ (M = Mo, W)

Francis Sécheresse*, Francis Robert, Saïd Manak
Laboratoire de Chimie des Métaux de Transition UA-CNRS 419, Université Pierre et Marie Curie, 4 Place Jussieu, 75252 Paris Cédex 05 (France)

Jean-Marie Manoli and **Claude Potvin**
Laboratoire de Réactivité de Surface et Structure, UA-CNRS 1106, Université Pierre et Marie Curie, 4 Place Jussieu, 75252 Paris Ceder 05 (France)

(Received July 1, 1990; revised November 5, 1990)

Abstract

Nucleophilic substitutions in the double cubane-like structures $[MS_4(CuCl)_5Cl_2]^{4-}$ (M = Mo, W) are complicated by elimination reactions. With NCS^- an edge-elimination process gave the $[MS_4(CuNCS)_4]^{2-}$ anion whereas a face-elimination by PPh_3 led to the monocubane structure $[MS_4(CuPPh_3)_3Cl]$. Substitution by bipyridine produced the lacunary $[MS_4Cu_{3.75}Cl_{1.75}bipy_2]$. The different species were characterized by X-ray diffraction studies.

Introduction

The tetrathiometallates MS_4^{2-} (M = Mo, W) are known to act as multidentate ligands to a wide variety of transition metal ions [1]. Among these compounds only two examples of double cubane-like structures have been chracterized, $[ReS_4(CuCl)_5Cl_2]^{3-}$ [2] and $[WS_4(CuCl)_5Cl_2]^{4-}$ [3].

A perspective view of the recently prepared molybdenum dicubane, shown in Fig. 1, confirms the open 12-atom cage. $[MS_4(CuCl)_5Cl_2]^{4-}$ is reactive, probably owing to the missing Cl'(4)–Cu(1) and Cu(1)–Cl(4) edges which make the close approach of nucleophilic reagents to the terminal CuCl groups or to the facial chloro bridges easier. Four active nucleophilic reagents were tested in this work: (i) the monodentate PPh_3 and NCS^- ligands, (ii) the bidentate 2,2′-bipyridine (bipy) and 1,10-phenanthroline (phen).

Experimental

Preparations of compounds

The complexes prepared here are air- and moisture-stable. Solvents and chemicals were used as purchased. Chemical analyses were performed by the Service Central d'Analyses du CNRS. Infrared spectra were recorded on a Perkin-Elmer 580 B spectrophotometer. UV-Vis spectra were obtained with a Uvikon 810 spectrophotometer.

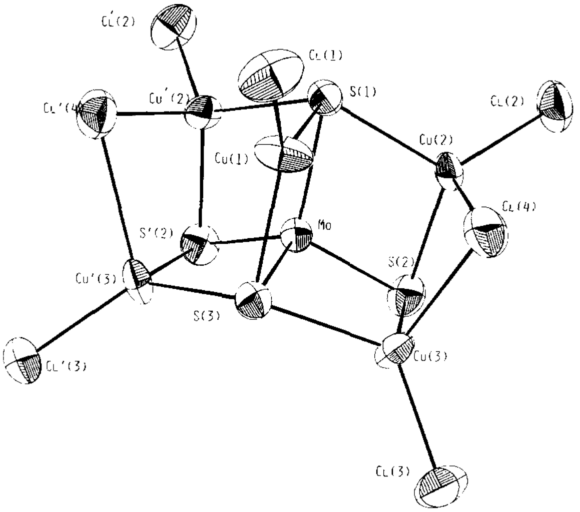

Fig. 1. Perspective view of the $[(CuCl)_5Cl_2MoS_4]^{4-}$ anion showing the atom labelling scheme. Half of the anion (primed atoms) is generated through a binary axis passing through Cu(1) and Cl(1).

$(NMe_4)_4[(CuCl)_5Cl_2MoS_4]$ (1)

This preparation completes our studies on the synthesis of double cubane-like structures [3]. The

---

*Author to whom correspondence should be addressed.

0020-1693/91/$3.50

route described here allows molybdenum dicubane as crystals of fair diffraction quality to be obtained. To a suspension of 0.093 g of $(NMe_4)_2(MoS_4)$ (0.25 mmol) in 25 ml of MeCN was added aerobically 0.075 g of CuCl (0.75 mmol). The mixture was stirred for 30 min and then filtered. The filtrate was kept at room temperature for 24 h. The violet crystals obtained were collected and washed with 20 ml of ether. The composition of **1** was established by IR and UV-Vis methods by comparison with the spectra of the homologous $(NMe_4)_4[(CuCl)_5Cl_2WS_4]$ [3] and by single X-ray analysis.

$[Cu_{3.75}Cl_{1.75}bipy_2WS_4]$ (2)

A solution of 0.090 g of bipyridine (bipy) (0.25 mmol) in 15 ml of acetonitrile was added to a solution of 0.059 g of $(NMe_4)_4[(CuCl)_5Cl_2WS_4]$ in 60 ml of acetonitrile. After storage for 8 hat room temperature the solution afforded red crystals which were collected and washed with ether. Electronic spectra: 432, 328(sh), 270(sh) nm, slightly soluble. IR spectra: 505, 470, 438 cm-' ν(W–S). The homologous Mo compound (2') was similarly obtained from 0.055 g of *1*. The composition and crystal structure of 2 were established by single-crystal X-ray analysis.

Addition of five equiv. of 1,10-phenantroline, previously dissolved in MeCN, to a solution of tungsten dicubane led after c. 24 h to $[WS_4Cu_2 phen_2]$, isolated as orange needles and identified by IR and UV-Vis spectra [4].

$[Cu_3(PPh_3)_3ClWS_4, CH_3CN]$ (3)

Compound 3 was obtained in this work as the product of the reaction of a solution of 0.040 g of PPh_3 (0.15 mmol) in 15 ml of MeCN with 0.059 g of $(NMe_4)_4[(CuCl)_5Cl_2WS_4]$ previously dissolved in 60 ml of MeCN. Storage for 24 h at room temperature afforded 0.040 g of yellow crystals. *Anal.* Calc. for $C_{56}H_{48}NP_3ClS_4Cu_3W$: C, 49.23; H, 3.51; S, 9.38; P, 6.81; Cl, 2.60; Cu, 13.96; W, 13.47. Found: C, 48.89; H, 3.31; S, 9.80; P, 7.02; Cl, 2.98; Cu, 14.42; W, 13.95%. The unsolvated species was prepared directly from WS_4^{2-}, CuCl and PPh_3 and characterized by Müller et *al.* [5].

$(NMe_4)_2[Cu_4(NCS)_4WS_4]$ (4)

A solution of 0.079 g of NH_4NCS (0.25 mmol) in 5 ml of acetonitrile was added to a solution of 0.059 g of $(NMe_4)_4[(CuCl)_5Cl_2WS_4]$ (0.05 mmol) in 60 ml of acetonitrile. After 24 h at room temperature a red precipitate was obtained. It was filtered off and washed with ether. The solid was identified as $(NMe_4)_2[Cu_4(NCS)_4WS_4]$ [6] by electronic and IR spectroscopies.

X-ray data collection and reduction

Suitable crystals of **1**, **2** and 3 were selected directly from the preparations. Diffraction studies were performed at room temperature on a Nonius CAD4 four-circle automated diffractometer with graphite monochromated Mo Kα radiation and a θ–2θ scan technique. The orientation matrix and unit cell parameters were determined by least-squares treatment of 25 machine-centered reflections. The intensities of three standard reflections were measured every 100 reflections and revealed no significant decay in intensities. The intensities were corrected for polarization and Lorentz effects. An empirical absorption correction based on azimuthal scan measurements was applied. Details concerning the intensity and data collection are given in Table 1.

Structure solution and refinement

Computations were performed by using SHELX76 [9] for 1 and 3 and CRYSTALS [10] programs for 2. Heavy-atom positions were obtained by the Patterson method. All remaining non-hydrogen atoms were located from successive least-squares refinements and difference Fourier maps. Anisotropic thermal parameters were introduced for Mo, W, Cu, S, P, N and C atoms. Final *R* factors are given in Table 1. Individual structural refinements are given for 2.

Results **and discussion**

Crystal structure of 1

The structure determination confirms that **1** is isostructural to $(NMe_4)_4[(CuCl)_5Cl_2WS_4]$ [3]. In both compounds the heavy metal Mo(W) and a CuCl group lie on the binary axis that generates a similar open 12-atom cage as shown in Fig. 1. The geometry about the Mo(W) is nearly tetrahedral, see Table 2. Five CuCl groups are bound to the MS_4 core (Cu-S 2.253(1)–2.366(2) Å) through double bridged copper atoms, the sixth edge of the MS_4 tetrahedron remaining uncoordinated. The overall geometry can be viewed as a distorted double cube with two long Cu(1)–Cl(4) distances, 3.173(2) Å for the Mo dicubane and 3.188(2) Å for the W dicubane. In both compounds the interatomic distances and angles are quite similar, consistent with the similar ionic radii of Mo(VI) and W(VI). See also 'Supplementary material'.

Infrared and electronic spectra

$(NMe_4)_2[MS_4(CuCl)_5Cl_2]$ (M = Mo, W) approximate C_{2v} symmetry so four IR-active vibrations (2a, b_1, b_2) are expected for the ν(M–S) stretching mode. Only two bands are observed in the corresponding

TABLE 1. Crystal data

Formula	$C_{16}H_{48}N_4Cl_7S_4Cu_5Mo$	$C_{20}H_{16}N_4Cl_{1.75}S_4Cu_{3.75}W$	$C_{56}H_{48}NP_3ClS_4Cu_3W$
Formula weight	1086	924.25	1365
Crystal system	monoclinic	monoclinic	triclinic
Space group	$C2/c$	$C2/m$	P i
a (Å)	21.552(4)	13.656(2)	11.895(4)
b (Å)	9.325(4)	19.069(5)	13.025(4)
c (Å)	19.561(3)	10.058(2)	20.296(3)
α (°)	90.0	90.0	75.24(2)
β (°)	92.71(2)	93.41(1)	85.64(2)
γ (°)	90.0	90.0	64.09(2)
V (Å^3)	3926	2614	2733
Z	4	4	2
ρ_{calc} (g cm-‘)	1.838	2.349	1.660
$F(000)$	2123.5	1825.6	1355.8
Systematic absences	hkl: $h+k=2n+1$; $h0l$: $l=2n+1$	hkl: $h+k=2n+1$	none
Diffractometer	CAD4 Enraf-Nonius	CAD4 Enraf-Nonius	CAD4 Enraf-Nonius
Radiation (graphite monochromator) λ Mo Kα (Å)	= 0.71069	0.71069	0.71069
Linear absorption coefficient (cm-‘)	35.49	76.85	34.32
Scan type	$\theta/2\theta$	$\theta/2\theta$	$\theta/2\theta$
Scan range (°)	$1.6+0.345$ tg θ	$0.80+0.345$ tg θ	$1.0+0.345$ tg θ
2θ limits (°)	3-50	3-50	3-50
Octants collected	$\pm h$, $+k$, $+l$	$\pm h$, $+k$, $+l$	$\pm h$, -k,+k, I
No. unique data collected	3437	2328	9579
No. unique data used $(F_o)^2>3\sigma(F_o^2))$	2672	1510	8211
No. refined parameters	169	175	337
$R=\Sigma(\|\|F_o\|-\|F_c\|\|)/\Sigma\|F_o\|$	0.038	0.038	0.0404
$R_w=[\Sigma w(\|F_o\|-\|F_c\|)^2/\Sigma wF_o^2]^{1/2}$	0.046	0.043	0.0404
Form factors		ref. 7	
Secondary extinction		yes [8]	

TABLE 2. Selected bond lengths (Å) and angles (°) for $(NMe_4)_2[MS_4Cu_5Cl_7]$[a]

Distances (A)			
Mo–S(1)	2.266(1)	W–S(1)	2.265(2)
Cu(1)–Cl(1)	2.146(2)	Cu(1)–Cl(1)	2.149(4)
Cu(2)–Cl(2)	2.173(2)	Cu(2)–Cl(2)	2.176(3)
Cu(3)–Cl(3)	2.205(2)	Cu(3)–Cl(3)	2.202(3)
Cu(1)–S(1)	2.253(1)	Cu(1)–S(1)	2.264(2)
Mo...Cu(1)	2.643(1)	W...Cu(1)	2.656(2)
Mo...Cu(2)	2.644(1)	W...Cu(2)	2.660(1)
Mo...Cu(3)	2.669(1)	W...Cu(3)	2.689(1)
Mo–S(2)	2.228(2)	W-S(2)	2.231(2)
Cu(1)...Cl(4)	3.173(2)	Cu(1)...Cl(4)	3.188(2)
Cu(2)–Cl(4)	2.774(2)	Cu(2)–Cl(4)	2.743(3)
Cu(3)–Cl(4)	2.531(2)	Cu(3)–Cl(4)	2.526(3)
Cu(2)–S(1)	2.312(1)	Cu(2)–S(1)	2.336(2)
Cu(2)–S(2)	2.230(2)	Cu(2)–S(2)	2.288(3)
Cu(3)–S(1)′	2.342(1)	Cu(3)–S(1)′	2.366(2)
Cu(3)–S(2)	2.282(2)	Cu(3)–S(2)	2.305(3)
Angles (°)			
S(1)–Mo–S(2)	109.33(5)	S(l)-W-S(2)	109.61(8)
S(1)–Mo–S(1)′	107.96(6)	S(l)-W-S(l)’	108.2(1)
Cu(1)...Mo...Cu(2)	83.06(2)	Cu(1)...W...Cu(2)	82.90(3)
Cu(2)...Mo...Cu(3)	75.22(3)	Cu(2)...W...Cu(3)	74.15(4)

(continued)

TABLE 2 ***(confirmed)***

Cu(2)...Mo...Cu(2)′	166.13(4)	Cu(2)...W...Cu(2)′	165.80(5)
Cl(1)–Cu(1)–S(1)	125.57(4)	Cl(1)–Cu(1)–S(1)	125.90(6)
S(1)–Cu(2)–S(2)	106.27(5)	S(1)–Cu(2)–S(2)	105.22(8)
Cl(2)–Cu(2)–S(1)	120.78(6)	Cl(2)–Cu(2)–S(1)	120.0(1)
Cl(2)–Cu(2)–S(2)	124.75(7)	Cl(2)–Cu(2)–S(2)	124.9(1)
Cl(2)–Cu(2)–Cl(4)	108.62(6)	Cl(2)–Cu(2)–Cl(4)	109.39(9)
S(1)–Cu(2)–Cl(4)	96.67(5)	S(1)–Cu(2)–Cl(4)	97.20(7)
S(2)–Cu(2)–Cl(4)	91.72(6)	S(2)–Cu(2)–Cl(4)	93.14(9)
Cl(1)–Cu(1)...Mo	54.43(4)	Cl(1)–Cu(1)...W	180.00
Cl(2)–Cu(2)...Mo	162.74(6)	Cl(2)–Cu(2)...W	161.37(9)
Cl(3)–Cu(3)...Mo	154.41(6)	Cl(3)–Cu(3)...W	153.86(8)
Mo-S(1)–Cu(1)	71.59(4)	W–S(1)–Cu(1)	71.81(7)
Mo-S(1)–Cu(2)	70.53(4)	w-S(1)-Cu(2)	70.62(7)
Mo–S(1)–Cu(3)′	70.77(3)	w-S(1)-Cu(3)	70.97(7)
Mo–S(2)–Cu(2)	71.98(5)	w-S(2)-Cu(2)	72.12(7)
Mo–S(2)–Cu(3)	72.55(5)	W-S(2)-Cu(3)	72.70(8)
S(1)–Mo–S(2)′	109.71(5)	S(1)-W-S(2)’	110.11(9)
S(2)–Mo–S(2)′	110.67(7)	S(2)-W-S(2)’	109.2(1)
Cu(1)...Mo...Cu(3)	83.40(2)	Cu(1)...W...Cu(3)	83.50(2)
Cu(2)...Mo...Cu(3)′	103.14(3)	Cu(2)...W...Cu(3)′	104.19(4)
Cu(3)...Mo...Cu(3)′	166.80(4)	Cu(3)...W...Cu(3)′	167.00(5)
S(1)–Cu(1)–S(1)′	108.86(8)	S(1)–Cu(1)–S(1)′	108.2(1)
S(2)–Cu(3)–S(1)′	105.23(6)	S(2)–Cu(3)–S(1)′	104.17(9)
Cl(3)–Cu(3)–S(1)′	121.81(6)	Cl(3)–Cu(3)–S(1)′	121.46(9)
Cl(3)–Cu(3)–S(2)	119.06(6)	Cl(3)–Cu(3)–S(2)	119.3(1)
Cl(3)–Cu(3)–Cl(4)	112.16(7)	Cl(3)–Cu(3)–Cl(4)	112.9(1)
S(1)–Cu(3)–Cl(4)	95.66(5)	S(1)–Cu(3)–Cl(4)	95.68(9)
S(2)–Cu(3)–Cl(4)	98.02(5)	S(2)–Cu(3)–Cl(4)	98.64(9)
Cl(4)–Cu(2)...Mo	88.62(4)	Cl(4)–Cu(2)...W	89.17(6)
Cl(4)–Cu(3)...Mo	93.40(4)	Cl(4)–Cu(3)...W	93.26(7)
Cu(1)–S(1)–Cu(2)	100.32(5)	Cu(1)–S(1)–Cu(2)	99.80(8)
Cu(1)–S(1)–Cu(3)′	100.52(5)	Cu(1)–S(1)–Cu(3)′	100.46(8)
Cu(2)–S(1)–Cu(3)′	126.82(6)	Cu(2)–S(1)–Cu(3)′	127.7(1)
Cu(2)–S(2)–Cu(3)	90.82(6)	Cu(2)–S(2)–Cu(3)	89.21(9)
Cu(3)–Cl(4)–Cu(2)	75.20(5)	Cu(3)–Cl(4)–Cu(2)	75.36(7)

[a] e.s.d.s are given in parentheses; the prime denotes an atom generated by the binary axis.

TABLE 3. Spectral data for $[MS_4(CuCl)_5Cl_2]^{2-}$ anions

Compounds	IR[a]		UV–Vis[b]
	ν(M–S)	ν(Cu–Cl)	
$[WS_4(CuCl)_5Cl_2]^{2-}$	450(s), 420(s)	340, 310, 290, 275, (m)	434 (4, 2) 328(sh), 308 (12, 5)
$[MoS_4(CuCl)_5Cl_2]^{2-}$	460(s), 448(m), 425(m)	340, 310, 290, 275, (m)	512 (3, 7), 360(sh) 308 (10, 5)

“Positions in cm-r, KBr pellets. [b] Wavelength in nm with molar absorptivities ($10^{-3}M^{-1}$ *cm-‘)*, dmf solutions.

region for the W dicubane, see Table 3, whereas three bands are present for the Mo dicubane, shifted to higher frequencies as usual for molybdenum. In the 350-250 cm^{-1} region where the ν(Cu–Cl) vibrations are expected the spectra of the two compounds are similar, as shown in Table 3.

The electronic spectra are dominated by the S-M charge transfers affected by the symmetry effects. In both compounds the position of the first band of absorption is shifted owing to the number of copper atoms coordinated to the central MS_4 core, 424 nm for $[WS_4(CuCl)_2]^{2-}$ and 434 nm for

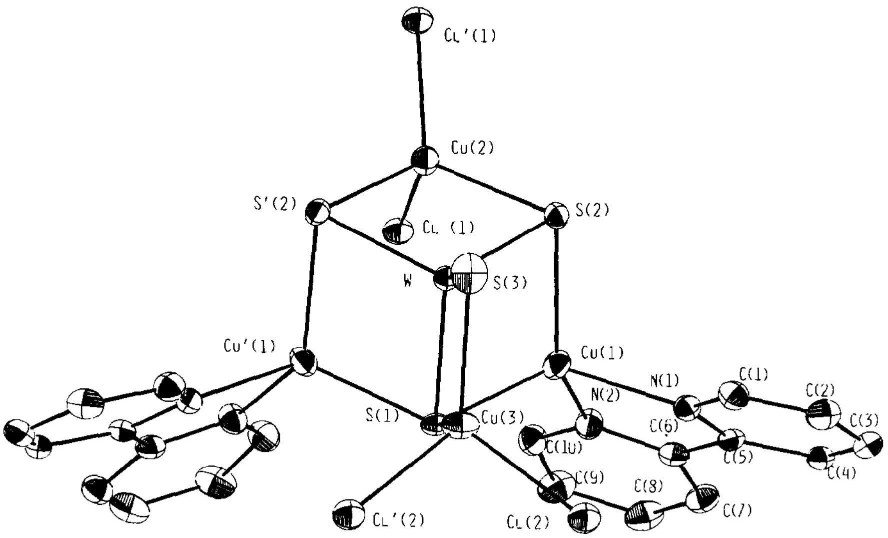

Fig 2. ORTEP drawing of the $[Cu_2Cl_2bipy_2WS_4]$ aggregate showing the atom numbering. Atoms W, Cu(2), Cu(3), S(l), S(3), Cl(l) lie in the mirror plane.

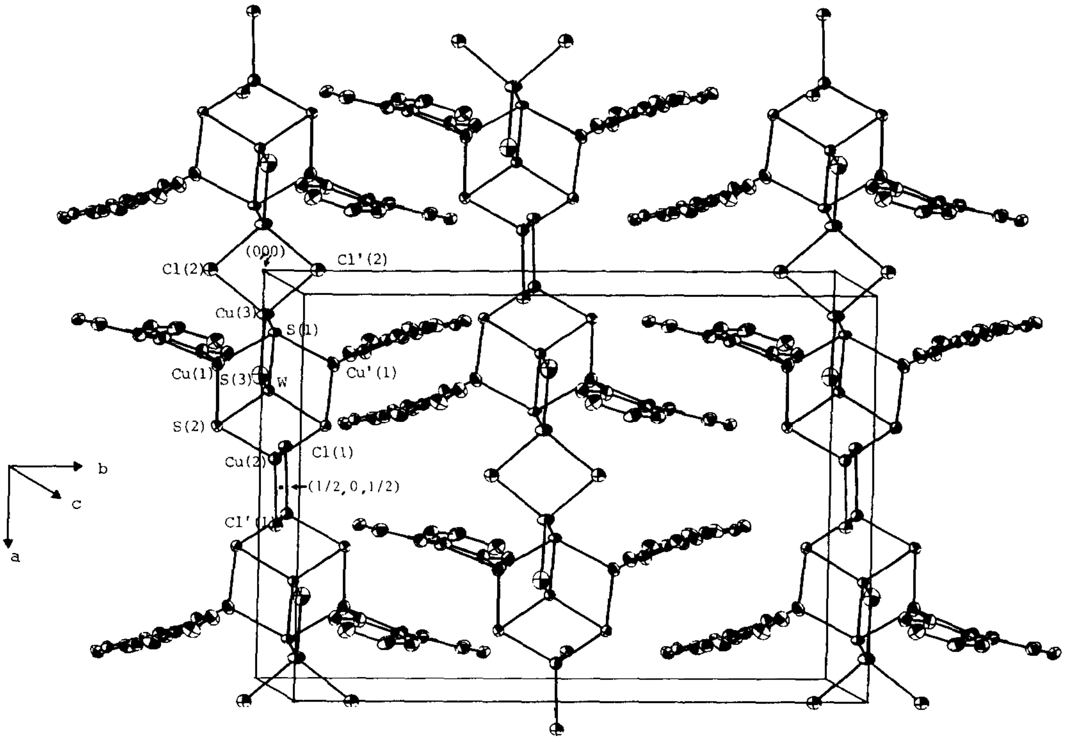

Fig. 3. View of 'the bidimensional arrangement along the [101] direction of the lacunary $[Cu_{3.75}Cl_{1.75}bipy_2WS_4]$.

$[WS_4(CuCl)_5Cl_2]^{4-}$, 502 nm for $[MoS_4(CuCl)_2]^{2-}$ and 512 nm for $[MoS_4(CuCl)_5Cl_2]^{4-}$.

Crystal structure of 2

The structure of **2** consists of neutral $[Cu_4Cl_2bipy_2WS_4]$ molecules containing the distorted WS_4 tetrahedral group. The tetrathiometallate acts as a tetradentate ligand towards four copper atoms as shown in Fig. 2 with W...Cu distances ranging from 2.641(1) to 2.700(2) Å. The Cl(l), Cu(2), W, S(3), Cu(3), S(1) atoms are located in the mirror plane. The Cu(2) and Cu(3) atoms are coordinated to the Cl(l) and Cl(2) atoms, respectively, and the

Cu(1) and Cu′(1) atoms related by the mirror are bonded each to a bipyridine ligand (angle between the two bipy cycles = 10.41”). The central core forms a distorted cube (W S(1) S(2) S’(2) Cu(1) Cu′(1) Cu(2)) with a missing corner and an additional face (S(3) Cu(3) S(1) W) lying in the mirror. The terminal Cl(1) and Cl(2) atoms serve as interaggregate bridges between the $WS_4Cu_4bipy_2$ units to form infinite chains running along the [101] axis as represented in Fig. 3. The Cl(2) and Cl′(2) atoms located on the C2 axis passing through the inversion centre at (0,0,0) are symmetrically disposed with respect to the mirror plane. Thus the Cl(2), Cu(3), Cl′(2) bridge is perpendicular to the mirror. The Cl(1) and Cl′(1) lying in the mirror are related by the C2 axis passing through the inversion centre at $(\frac{1}{2},0,\frac{1}{2})$ (see Fig. 3) so the corresponding Cl(l), Cu(2), Cl′(1) bridge is contained in the mirror. The in-plane Cu(2)–Cl(1) and Cu(2)–Cl′(1) distances are unsymmetrical (2.256(4) and 2.559(4) Å) and quite different from the out-plane Cu(3)–Cl(2) separation of 2.349(4) Å (see Table 5). Both values remain comparable with the bridging CuCl distances observed in the $[(WS_4Cu_4Cl_4)_2]^{4-}$ dimer [11]. No graphitic interactions exist between two adjacent chains consistent with C-C interchain distances larger than 3.6 Å.

The W-S(3) bond is short, 2.128(4) Å, closer to a terminal W=S bond than to a W-S-Cu bridge. This observation, together with the evidence in the Fourier-difference map processed at $R = 0.07$ of a residual peak at 0.7 Å from the S(1) atom and the significantly high value of the isotropic thermal parameter of the Cu(3) and Cl(2) atoms, led us to postulate a lack of CuCl. With this hypothesis the occupancy factors of the Cu(3) and Cl(2) atoms converged to 0.75 and occupations values of 0.75 and 0.25 were found for the S(1) and S(l)* disordered positions, respectively giving a R index of 0.038. In the additional face (W S(3) Cu(3) S(1)) a Cu(3) Cl(2) molecule is statistically missing every four units (occupancy 0.75) leading to the formation of the

TABLE 4. Fractional atomic coordinates for $[WS_4Cu_{3.75}Cl_{1.75}(C_{10}H_8N_2)_2]^a$

Atom	x/a	y/b	z/c	U_{eq}	Occupancy
W(1)	0.28570(4)	0.0000	0.17000(6)	0.0332	1.00
Cu(1)	0.2130(1)	0.10099(6)	0.3154(1)	0.0482	1.00
Cu(2)	0.4409(1)	0.0000	0.3493(2)	0.0439	1.00
Cu(3)	0.1073(2)	0.0000	0.0490(3)	0.0501	0.75
S(1)	0.1394(4)	0.0000	0.2720(6)	0.0329	0.75
S(1)*	0.126(1)	0.0000	0.207(2)	0.0102	0.25
S(2)	0.3676(2)	0.0951(1)	0.2448(3)	0.0380	1.00
S(3)	0.2618(4)	0.0000	−0.0410(4)	0.0625	1.00
Cl(1)	0.3969(2)	0.0000	0.5931(3)	0.0439	1.00
Cl(2)	0.0000	−0.0940(3)	0.0000	0.0544	0.75
N(1)	0.1577(5)	0.1989(4)	0.2449(8)	0.0408	1.00
N(2)	0.1728(7)	0.1422(5)	0.4883(9)	0.0476	1.00
C(1)	0.1550(8)	0.2250(6)	0.123(1)	0.0516	1.00
C(2)	0.1312(8)	0.2943(7)	0.096(1)	0.0551	1.00
C(3)	0.1126(8)	0.3383(6)	0.198(1)	0.0544	1.00
C(4)	0.1156(7)	0.3120(6)	0.325(1)	0.0445	1.00
C(5)	0.1382(6)	0.2428(5)	0.349(1)	0.0375	1.00
C(6)	0.1397(7)	0.2087(6)	0.482(1)	0.0410	1.00
C(7)	0.1068(7)	0.2415(6)	0.592(1)	0.0498	1.00
C(8)	0.1041(9)	0.2053(8)	0.709(1)	0.0607	1.00
C(9)	0.1348(9)	0.1360(8)	0.715(1)	0.0595	1.00
C(10)	0.1709(9)	0.1073(6)	0.604(1)	0.0528	1.00
				U_{iso}	
H(1)	0.1697	0.1945	0.0496	0.06(1)	
H(2)	0.1280	0.3112	0.0070	0.06(1)	
H(3)	0.0966	0.3865	0.1792	0.06(1)	
H(4)	0.1026	0.3422	0.3977	0.06(1)	
H(7)	0.0845	0.2893	0.5868	0.06(1)	
H(8)	0.0825	0.2278	0.7874	0.06(1)	
H(9)	0.1295	0.1090	0.7942	0.06(1)	
H(10)	0.1966	0.0601	0.6091	0.06(1)	

[a] e.s.d.s in parentheses refer to last digit. Asterisk indicates a disordered position.

TABLE 5. Selected interatomic distances (Å) and angles (°) for $[WS_4Cu_{3.75}Cl_{1.75}(C_{10}H_8N_2)_2]$[a]

Distances (Å)			
W(1)-S(1)	2.299(5)	W(1)-S(1)*	2.23(2)
W(1)-S(3)	2.128(4)	W(1)-S(2)	2.237(2)
W(1)-Cu(1)	2.646(1)	W(1)-Cu(2)	2.700(2)
W(1)-Cu(3)	2.657(2)		
Cu(2)-Cl(1)	2.559(4)	Cu(2)-Cl(1)	2.256(4)
Cu(2)-S(2)	2.296(3)		
Cu(3)-S(1)	2.260(7)	Cu(3)-S(3)	2.344(6)
Cu(3)-Cl(2)	2.349(4)		
Cu(1)-S(1)	2.204(3)	Cu(1)-S(1)*	2.481(9)
Cu(1)-S(2)	2.269(3)		
Cu(1)-N(1)	2.119(8)	Cu(1)-N(2)	2.015(9)
Angles (°)			
Cu(1)-W(1)-Cu(1)	93.39(6)	Cu(1)-W(1)-Cu(2)	86.34(4)
Cu(3)-W(1)-Cu(1)	165.39(7)	Cu(1)-W(1)-Cu(3)	83.65(5)
S(3)-W(1)-S(1)	111.0(2)	S(2)-W(1)-S(1)	106.3(1)
S(2)-W(1)-S(3)	112.3(1)	S(2)-W(1)-S(2)	108.3(1)
S(3)-W(1)-S(1)*	94.1(5)	S(2)-W(1)-S(1)*	114.7(2)
S(2)-Cu(1)-S(1)	108.4(1)	N(1)-Cu(1)-S(1)	123.6(3)
N(2)-Cu(1)-S(1)	111.5(3)	N(1)-Cu(1)-S(2)	105.0(2)
N(2)-Cu(1)-S(2)	126.6(3)	N(2)-Cu(1)-N(1)	80.5(3)
S(2)-Cu(1)-S(1)*	104.6(5)	N(1)-Cu(1)-S(1)*	112.6(3)
N(2)-Cu(1)-S(1)*	122.3(6)		
Cl(1)-Cu(2)-Cl(1)	92.1(1)	S(2)-Cu(2)-Cl(1)	108.5(1)
S(2)-Cu(2)-Cl(1)	120.83(9)	S(2)-Cu(2)-S(2)	104.4(1)
S(3)-Cu(3)-S(1)	104.9(2)	Cl(2)-Cu(3)-S(1)	106.9(1)
Cl(2)-Cu(3)-S(3)	118.9(1)	Cl(2)-Cu(3)-Cl(2)	99.5(2)
Cu(3)-S(1)-W(1)	71.3(2)	Cu(1)-S(1)-W(1)	72.0(1)
Cu(1)-S(1)-Cu(3)	104.8(2)	Cu(1)-S(1)-Cu(1)	121.8(3)
Cu(1)-S(1)*-W(1)	68.1(3)	Cu(1)-S(1)*-Cu(1)	101.8(5)
Cu(2)-S(2)-W(1)	73.10(8)	Cu(1)-S(2)-W(1)	71.94(8)
Cu(1)-S(2)-Cu(2)	106.5(1)	Cu(3)-S(3)-W(1)	72.7(2)
Cu(2)-Cl(1)-Cu(2)	87.9(1)	Cu(3)-Cl(2)-Cu(3)	80.5(2)

[a] Asterisk indicates a disordered position.

terminal W=S(3) double bond. A fairly experimental confirmation of this postulated lack of CuCl was obtained from the IR spectra of 2 and 2': a weak band is observed at 505 cm^{-1} characteristic of the vibration of a W=S double bond [12].

The distribution of the S(1) atom in two different sites is probably related with the change of the coordination of the sulfur atom which decreased from four (in dicubane structure) to three (in monocubane structure) after the removal of Cu(3).

The structure can then be viewed as $[Cu_{3.75}Cl_{1.75}bipy_2WS_4]_4$ chains statistically distributed along the [101] direction (Fig. 3) generating a lacunary structure.

Atom positional parameters for the structure are given in Table 4; selected interatomic distances and angles are presented in Table 5. See also 'Supplementary material'.

Crystal structure of 3

Except for the additional CH_3CN molecule the structure of *3* is similar to that previously described by Miiller *et al.* [5]. Results related to the structure refinements are given in Table 1. See also 'Supplementary material'.

Discussion of the reactions

In the dicubane structure, represented in Fig. 1, the four copper atoms Cu(2), Cu'(2), Cu(3), Cu'(3) are tetrahedrally coordinated so only substitution or elimination reactions are expected.

By reaction with NCS$^-$ anions the four terminal chlorides Cl(2), Cl'(2), Cl(3), Cl'(3) are symmetrically substituted while the trigonal Cu(1) atom lying on the binary axis is removed.

The reaction can be viewed as a nucleophilic substitution of the terminal chloro ligands complicated by an 'edge-elimination' as represented in Fig. 4(a). The main consequences of this scheme are that the faces containing the binary axis and the two bridging chlorines are removed. The product of the reaction was identified as the tridimensional

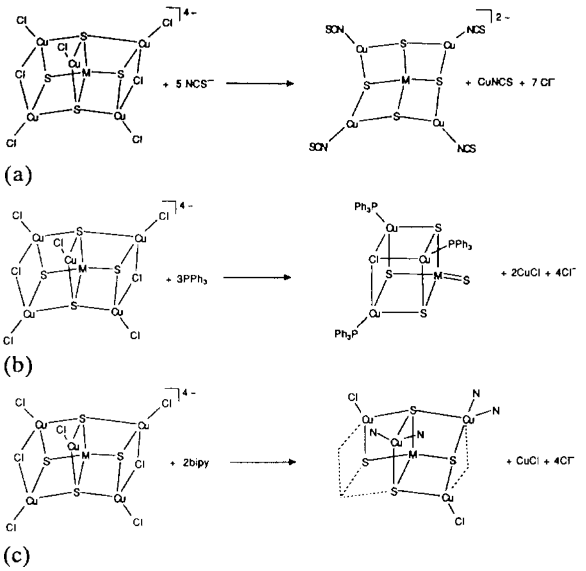

Fig. 4. Derivatives of the double cubane-like structure: (a) edge-elimination scheme in dicubane structure; (b) face-elimination in dicubane structure giving a cubane-like geometry; (c) bipy substitution in $[(CuCl)_5Cl_2MS_4]^{4-}$ anion.

polymer $[WS_4Cu_4(NCS)_4]^{2-}$ (4) previously obtained [6] by direct addition of CuCl to $(NMe_4)_2MS_4$.

With PPh_3 the substitution of the terminal chlorines is accompanied by the 'face-elimination' of the two Cu'(2)Cl'(2), Cu'(3)Cl'(3) groups and the bridging Cl'(4) chlorine, see Fig. 4(b). The mean plane (containing the trigonal Cu(1) atom) and the Cl(4) bridging chlorine are retained to complete the geometry of the monocubane-like structure of 3.

Figure 4(c) illustrates the reaction of **1** with bipyridine. The substitution of the terminal Cl(1) and Cl(2) atoms by two molecules of bipyridine is accompanied by the elimination of the two Cl(4) and Cl'(4) bridging.atoms and of the Cu'(3)Cl'(3) group. The substitution of the two terminal chloro-monodentate ligands by two bipy molecules results in the elimination of the two chloro bridges to respect the tetracoordination of Cu(1) and Cu(2). Then the elimination scheme is intermediate between a face- and an edge-elimination.

Supplementary material

Anisotropic thermal parameters (Table SS), non-selected bond distances and angles in the bipy ligand (Table S4), complete structure results for **1** (Tables S1–S3), a set of numeric data (Tables S6 to S9) and an ORTEP drawing for 3 are available from author F.S. on request.

References

1 A. Miiller, E. Dicmann, R. Jostes and H. Bögge, *Angew. Chem., Int.* Ed. *Engl.,* 20 (1981) 934.

2 A. Miiller, E. Krickmeyer and H. Bögge, *Angew. Chem., Int. Ed. Engl., 25 (1986) 990.*

3 F. Sécheresse, J. M. Manoli, C. Potvin and S. Marzak, *J. Chem. Soc., Dalton Trans., (1988) 3055.*

4 *C.* Potvin, J. M. Manoli, F. Sécheresse and S. Marzak, *Inorg. Chim. Acta, 134 (1987) 9.*

5 A. Miiller, H. Bögge and U. Schimanski, *Inorg. Chim. Acta,* 69 (1983) 5.

6 J. M. Manoli, C. Potvin, F. Stcheresse and S. Marzak, *J. Chem. Soc., Chem. Commun.,* (1986) 15.57.

7 *International Tables for X-ray Crystallography,* Vol. IV, Kynoch Press, Birmingham, U.K., 1974, pp. 99–101.

8 A. C. Larson, *Crystallographic Computing,* Munksgaard, Copenhagen, 1970, pp. 291.

9 G. M. Sheldrick, *SHELX76,* crystal solving package, University of Cambridge, U.K., 1976.

10 D. J. Watkin, J. K. Carruthers and P. W. Betteridge, *An Advanced Crystallographic Program System,* Chemical Crystallography Laboratory, University of Oxford, U.K., 1986.

11 W. Clegg, C. D. Scattergood and C. D. Garner, *Acta Crystallogr., Sect C,* 43 (1987) 786.

12 A. Miiller, W. Jaegermann and W. Hellmann, *J.* Mol. *Struct.* ZOO (1983) 559.